TECHNICAL ARTICLE

Microstructural Evolution and Mechanical Properties of Vacuum Brazed TC4 Titanium Alloy Joints with Ti-Zr-Ni Filler Metal

Min Liang, Youqiong Qin, Danfeng Zhang, and Feng Zhao

Ti-6Al-4V alloy was brazed in vacuum using self-designed and non-copper Ti-38Zr-24Ni (wt.%) filler metal. The microstructural evolution and mechanical properties of the joints were researched. Ni and Zr atoms diffused into based material and led to β-Ti transformation, which formed the diffusion zone. Its microstructure was α-Ti and (Ti, Zr)$_2$Ni eutectoid structures and remained based material. The interface zone was formed through isothermal solidification, which was composed of α-Ti and (Ti, Zr)$_2$Ni by eutectoid transformation. The center zone was comprised of big block brittle (Ti, Zr)$_2$Ni IMCs and some tiny phases: α-Ti and (Ti, Zr)$_2$Ni by hypoeutectic and following eutectoid transformation. The maximum shear strength was 673MPa at 930°C for 45 min. The weak area was the center zone. Cracks initiated and propagated in the brittle (Ti, Zr)$_2$Ni IMCs in the center zone and may be hindered by α-Ti which exhibited the mixed quasi-cleavage and cleavage fractures.

1. Introduction

TC4 titanium alloy (Ti-6Al-4V, wt.%) has been widely used because of its excellent characteristics, such as high specific strength and good corrosion resistance. It is a typical duplex alloy which contains hexagonal close-packed (hcp) α phase and body-centered cubic (bcc) β phase (Ref 1).

Fusion welding (Ref 2, 3) and solid-state welding (Ref 4, 5) have been successfully applied to join TC4. However, to some complex components, brazing, especially vacuum brazing is more suitable to join them on account of the merits of low brazing temperature, slight deformation and free from gas contamination (Ref 6).

Al-based, Ag-based and Ti- (or Ti-Zr-based) alloys are the common filler metals used to braze titanium and titanium alloy (Ref 7, 8). However, the service temperature with Al- and Ag-based filler metal is not up to 500°C. Moreover, the formation of intermetallic compound in brazed joints led to low strength and ductility (Ref 9). Compared to Al- and Ag-based filler metal, the brazed joints with Ti-(or Ti-Zr based) filler metal

Min Liang, Danfeng Zhang, and **Feng Zhao**, School of Material Engineering, Shanghai University of Engineering Science, Shanghai 201620, People's Republic of China; and **Youqiong Qin**, School of Material Engineering, Shanghai University of Engineering Science, Shanghai 201620, People's Republic of China; and Shanghai Collaborative Innovation Center of Laser Advanced Manufacturing Technology, Shanghai University of Engineering Science, Shanghai 201620, People's Republic of China. Contact e-mail: qyqqin@163.com.

have good performances, such as good corrosion resistance or high temperature strength (Ref 10, 11). This is because the composition of the brazed joints is similar to the based metal after their alloying of filler metal and based material, which leads to the strength, corrosion resistance and thermal resistance of joint close to the based material.

For the titanium alloy, if the brazing temperature is above the restrictive temperature (β transus temperature), the strength of the based material would deteriorate (Ref 12, 13). Therefore, some melting point depressants (MPDs) (such as Zr, Cu, Ni, and Be) are added to the Ti-based filler metal to reduce the fusing point of the filler metal. Zr is a preferable MPD to add into Ti because of the low melting point of Ti-Zr and their infinite solid solution between Ti and Zr. Moreover, Ni and Cu are used as MPDS, too, which can primarily reduce the fusing point of the filler metal (Ref 14). However, it was found that the concentration of Cu in the center led to the increased brittleness of the brazed joint and deteriorated the mechanical properties. Botstein et al. (Ref 15) reported that λ-Cu$_2$(Ti,Zr) and γ-(Ti,Zr)$_2$Cu intermetallic phases existed in middle of brazing seam during the brazing of TC4 with Ti-25Zr-50Cu (wt. %). Therefore, the strength of the brazed joint was very low as result of the formation of IMCs containing Cu. Shapiro et al. (Ref 16) showed that the quantity of Cu in the joints ought not to 10wt.%. A new filler metals containing no Cu or low Cu were suggested to braze titanium alloy. Based on the above, Ti-Zr-based filler metal containing Cu possesses low melting point, but the brazed joint had low strength and corrosion resistance. Therefore, the brazing characteristics with Ti-Zr-Ni with no Cu or low Cu should be deeply discussed. In our experiment, a Ti-Zr-based filler metal containing no Cu (Ti-38Zr-24Ni, wt.%) was self-designed and manufactured on the basis of Ti- Zr- Ni phase diagram. The physical properties of the filler metal were tested. The microstructure and strength of the joint were studied with different holding times and brazing

temperatures. Simultaneously, the microstructure transformation and fracture pattern of the joints were investigated, too.

2. Experimental Procedures

TC4 titanium alloy was employed as based material. Its chemical composition was Ti-6Al-4V (wt.%). Figure 1 displays the microstructure of TC4. It contains α-Ti phases (blocky) and around β-Ti phases. Ti-38Zr-24Ni (wt.%) was self-designed and prepared. The processing is: Firstly, 99.99% pure Ti, Zr and Ni blocks were weighed by mass ratio. Then, they were melted three times by an electric arc furnace equipped with magnetic stirring. A homogeneous alloy ingot was obtained. The melting region of the filler metal was about 847-869°C obtained by differential scanning calorimetry (DSC) with heating speed (20°C/min).

TC4 titanium alloy was cut into the dimensions of 20mm×15mm×5mm and 10mm×7.5mm×5mm, respectively. The filler metal was also cut into small pieces.

Before brazing, abrasive papers from 80# to 1000# were used to grind the specimens of the based material and the pieces of the filler metal. In the following, acetone was adapted to wash them for 15min. At last, air blowing was to dried them. TC4 was overlapped. The small specimen of TC4 was put in the middle of the large specimen for shear strength testing. Three small films (about 1mm × 1mm) of $100 \mu m$ Ti foil were put into the brazed joint to control the brazing clearance. The small pieces of filler metal were placed in the corner of the brazing seam. According to the volume of the brazing seam (V) and the density of the filler metal (ρ). The volume was obtained by $V=L$(length)×W(width)×H(height). A suitable weight (m=ρV) of the filler metal species was adopted. Figure 2 gives the installation schematic diagram.

In this experiment, the brazing temperature varied from 900 to 990°C. Meanwhile, the holding time differed from 5 to 45min. Table 1 shows the variable parameters. After brazing, the metallographic sample was ground, polished and etched using 3ml HF+36mlHNO$_3$+100mlH$_2$O. The intersecting surface was analyzed by a scanning electron microscope (SEM). The composition of phases was determined by an energy dispersive spectrometer (EDS). As shown in Fig. 2(c), AG-25TA strength testing device was used to measure the shear strength. The compressing rate was 1mm/min. The average shear strength was from three samples in every case. The melting point was obtained by DSC differential scanning calorimetry. The phases in the fracture surface were investigated by X Perp PRO x-ray diffraction (XRD). Cu Kα was
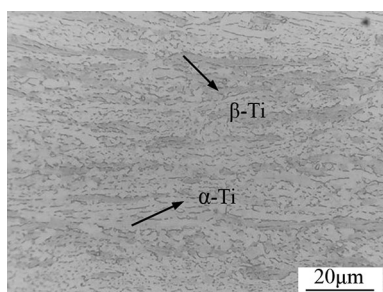
selected as the source of x-rays with a scan range of 0-80° and a speed of 8°/min.

3. Results

3.1 Microstructure of the Brazed Joints

The typical interfacial microstructure of the joint at 930°C/10 min is revealed in Fig. 3. Its elemental distribution from the interface zone to based material is also given in Fig. 3. As shown in Fig. 3(a), no defects were found in the joint. The width of the brazing seam was about $180 \mu m$. The factual width was largely wider than the predetermined level owing to the diffusion and reaction between the based material and filler metal. The joint contained three different zones: diffusion zone, interface zone and center zone, respectively (marked as I, II and III). Zone I was close to the based material. Zone III was in the center of the brazing seam, which consisted in white phases and lamellar structure with black and white. Zone II was between zone I and zone III.

To thoroughly analyze the phases, the chemical composition of every phase is listed in Table 2. The major element content distributions (the white line given in the picture from the based material to zone III) are given in Fig. 3(d). From the result of elemental line scanning in Fig. 3(d), Ni and Zr diffused into the TC4-based material and reacted with TC4, which formed zone I. From the local enlargement of the Ni element distribution in Fig. 3(d), Ni in zone I was more than that in zone II and the distribution of Ni in zone I was inhomogeneous. This can be used to distinguish the diffusion zone and the interface zone. In zone I, the black phase (point A_1) was mainly composed of Ti. It was α-Ti of original based material. The white phase (point A_2) was mainly composed of 40.83at.% Ti, 29.01at.% Zr and 20.87at.% Ni. The atomic percentage of (Ti+Zr) and Ni was about 2:1. Therefore, the white phase was (Ti,Zr)$_2$Ni intermetallic compound, corresponding to the result in references (Ref 17, 18). During the brazing process, some Ni and Zr diffusion into the TC4-based material at first and the eutectoid transformation occurred in the following. So zone I was α-Ti + (Ti,Zr)$_2$Ni.

In zone II, the chemical composition of the black phase (B_1) and the white phase (B_2) was similar to the A_1 and A_2, respectively. Nevertheless, the black and white phase presented the lamellar structure. During the processing of brazing, Ti fused into the melted filler metal from TC4-based material. When the cooling process began, β-Ti was precipitated from the melted filler metal along the solid-based material. Therefore, α-Ti + (Ti,Zr)$_2$Ni lamellar structure was formed in the following eutectoid transformation.

In zone III, it was composed of the big block white phase and the lamellar structure with black and white. The big block white phase (point C_1) consisted of 35.01at.% Ti, 30.48at.% Zr and 27.48at.% Ni. From the Ti-Zr-Ni phase diagram, it was (Ti,Zr)$_2$Ni. There are two sizes of laminar structure (the big size (C_2+C_3) and the small size (C_4+C_5)), which can be obviously seen at other brazing parameters (such as 960°C/10min). In the two sizes of laminar structure, the black phase (points C_2 and C_4) mainly consisted of Ti and Zr. It was α-Ti, and the white phase (point C_3 and C_5) mainly consisted of Ti, Zr and Ni, it was similar to point B_2, so it was (Ti,Zr)$_2$Ni. According to the microstructural morphology and Ti-Zr-Ni phase diagram,

β-Ti

α-Ti

20μm

Fig. 1 Microstructure of TC4
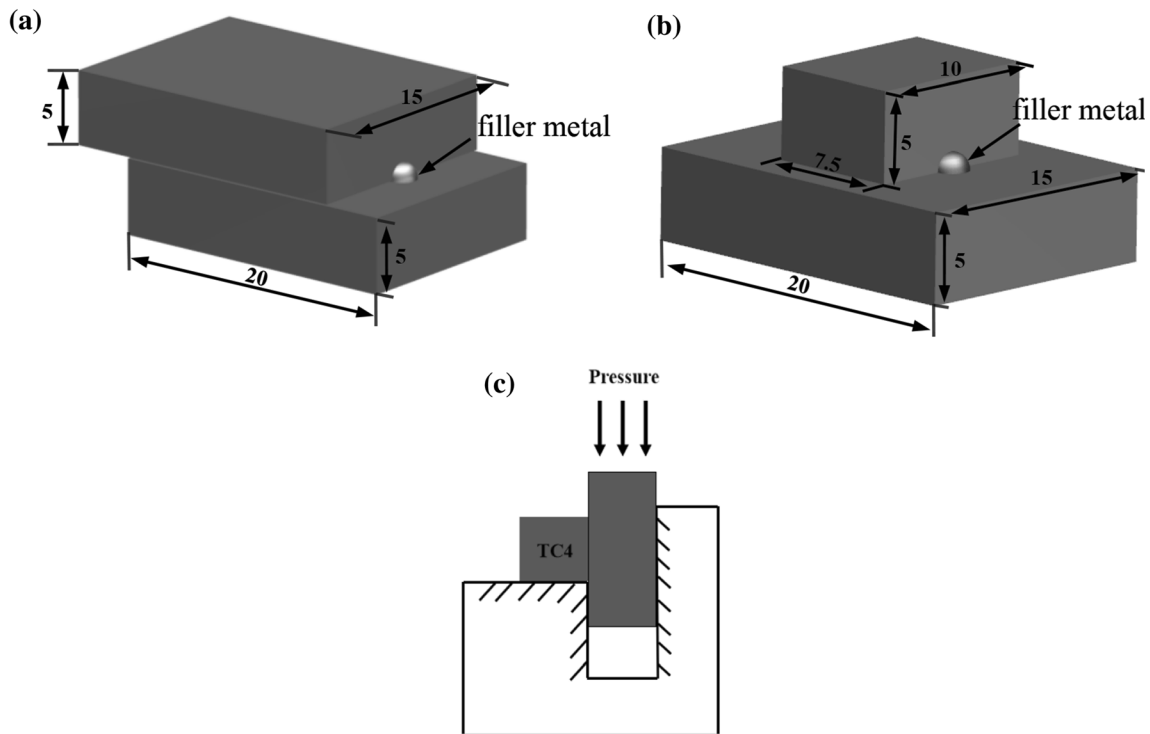
Fig. 2 Schematic diagram of brazed specimen assembly (Length unit: mm): (a) microstructure analysis specimen; (b) shear strength analysis specimen. (c) sectional view of shear strength test

Table 1 The brazing parameters in the experiment

	Brazing temperature, °C	Holding time, min
No.1	900	10
No.2	930	10
No.3	960	10
No.4	990	10
No.5	930	5
No.6	930	20
No.7	930	45

during the cooling process, β-Ti was also precipitated by the fused filler metal at its center for non-equilibrium solidification, which formed the big-sized laminar structure $(L \rightarrow β\text{-Ti}+L)_{hypoeutectic}$. Then, the temperature dropped to the eutectic point. The eutectic transformation occurred $(L \rightarrow β\text{-Ti}+ (Ti,Zr)_2Ni)_{eutectic}$. The big block white phase $(Ti,Zr)_2Ni$ formed. Finally, both of the precipitated β-Ti and eutectic transformation β-Ti transformed to the laminar structure with black and white by eutectoid transformation $(β\text{-Ti} \rightarrow α\text{-Ti}+ (Ti,Zr)_2Ni)_{eutectoid}$. The size of the precipitated phase was usually more bigger than the eutectic transformation phase due to the longer crystallization time. The eutectic pattern between the white phase $(Ti,Zr)_2Ni$ and the small size of the laminar structure can also support this point (seemed in Fig. 3a). The eutectic pattern was more obvious in the following images with other brazing parameters (such as 960°C/10min).

Figure 4 displays the microstructure changes with variable parameters. The whole thickness of the brazing seam increased with the increase in brazing temperature or holding time. Especially at high brazing temperature of 990°C or long

holding time (45min), the whole thickness of the brazing seam was up to 320 and 230μm, respectively. Meanwhile, the breadth of zone III deduced, but the thickness of zone I and zone II increased at the raising of brazing temperature or the prolonging of holding time. In zone III, the quantity of the eutectoid transformation phase also increased with raising parameters, but when the temperature was very high (such as 990°C) and the holding time was very long (such as 45min), the amount of the eutectoid transformation phase was seemed to decrease. However, it was not difficult to see that the thickness of zone III was low, and the proportion of the eutectoid transformation phase (zone III) was also large and the size of $(Ti,Zr)_2Ni$ was lessened by the interrupting of the eutectoid transformation phase.

Raising the brazing temperature, the diffusion and dissolution between TC4 and the filler metal intensified. Therefore, more Ni and Zr diffused into TC4 formed zone I (diffusion zone). The thickness of zone I increased. Meanwhile, more Ti from based material dissolved into the melted alloy. The composition of the melted alloy was toward hypoeutectic alloy with a high proportion of Ti. In the following cooling process, more β-Ti formed at higher brazing temperature. That was the reason why zone I was thicker. The amount of the precipitation phase in zone III was more at the higher brazing temperatures. However, if the brazing temperature was so high (Fig. 4c), the strong diffusion led to little residual Ni and Zr in the center. The thickness of zone III was small. Moreover, the melted hypoeutectic alloy at higher brazing temperature led to more proportion of the eutectoid transformation phase in zone III. Furthermore, it should be noted that widmanstätten microstructure was obtained at high brazing temperature (seemed in Fig. 4c) in zone I, if the brazing temperature was so high than the restrictive temperature (about 985°C). In the processing of
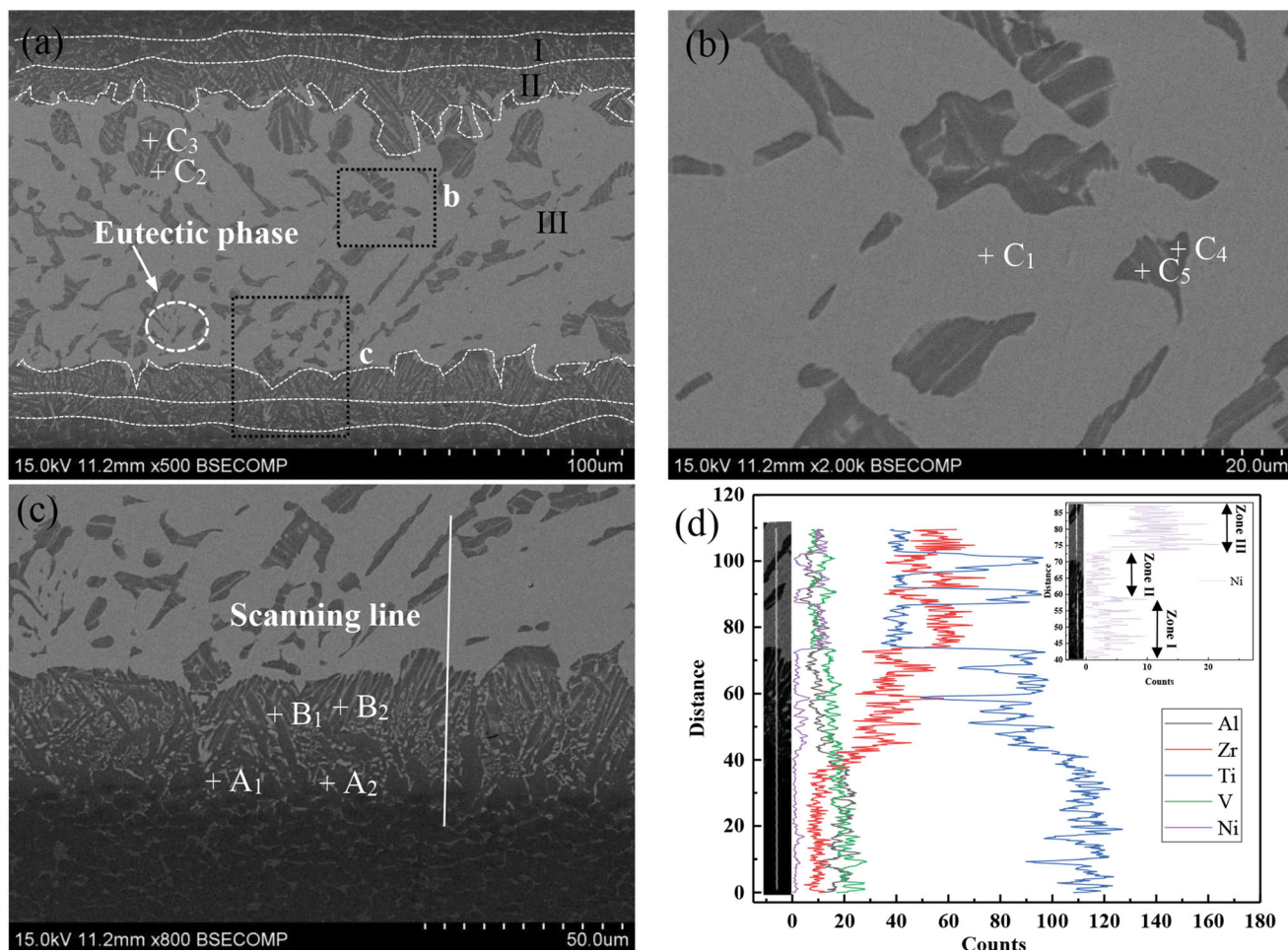
Fig. 3 Microstructures and major element content distribution of brazed joint: (a) microstructure of the brazed joints at 930°C for 10min, (b) and (c) high-magnification images of zone I and Zone II+III and (d) distribution of elements along the direction of the white line in (c)

Table 2 Average chemical composition (at.%) analysis of different zones of the brazed joint in Fig. 3

| Zone	Position	Ti	Zr	Ni	V	Al	Possible phase
I	A_1	83.35	2.64	0.36	1.55	12.10	α-Ti (high Ti concentration)
I	A_2	36.83	24.01	29.87	3.06	6.23	$(Ti,Zr)_2Ni$
II	B_1	78.08	10.04	0.90	0.60	10.38	α-Ti
II	B_2	34.44	30.06	27.71	3.19	4.60	$(Ti,Zr)_2Ni$
III	C_1	33.01	30.48	30.23	2.57	3.71	$(Ti,Zr)_2Ni$
III	C_2	77.86	10.30	8.48	0.94	2.42	α-Ti
III	C_3	32.73	31.11	29.77	3.16	3.23	$(Ti,Zr)_2Ni$
III	C_4	72.96	13.20	10.38	1.94	1.52	α-Ti
III	C_5	31.85	31.01	30.75	3.26	3.13	$(Ti,Zr)_2Ni$

brazing, Ni atoms from the liquid diffused into the original based material. Some based material transformed to β phase because of Ni (β-Ti stabilized element). In the following cooing process, acicular α phase may be obtained due to its probable nucleation and growth along $[110]_\beta$ directions. Meanwhile, untransformed β phases were left (Ref 19). That is to say, the widmanstätten microstructure formed at zone I with temperature up to the β transus temperature.

Similarly, increasing the holding time, the dissolution and diffusion time between TC4 and the filler metal lengthened. The breadth of zone I and II increased, but zone III decreased.

Meanwhile, the amount of the eutectoid transformation phase in zone III was more due to a longer dissolution time by non-equilibrium solidification.

3.2 Mechanical Properties of the Brazed Joints

The variation of average shear strength at variable parameters is shown in Fig. 5. The shear strength of TC4-TC4 brazed joint slowly increased from 900 to 990°C brazing temperature, as shown in Fig. 5(a). Similarly, the shear strength of the brazed joints increased when the holding time
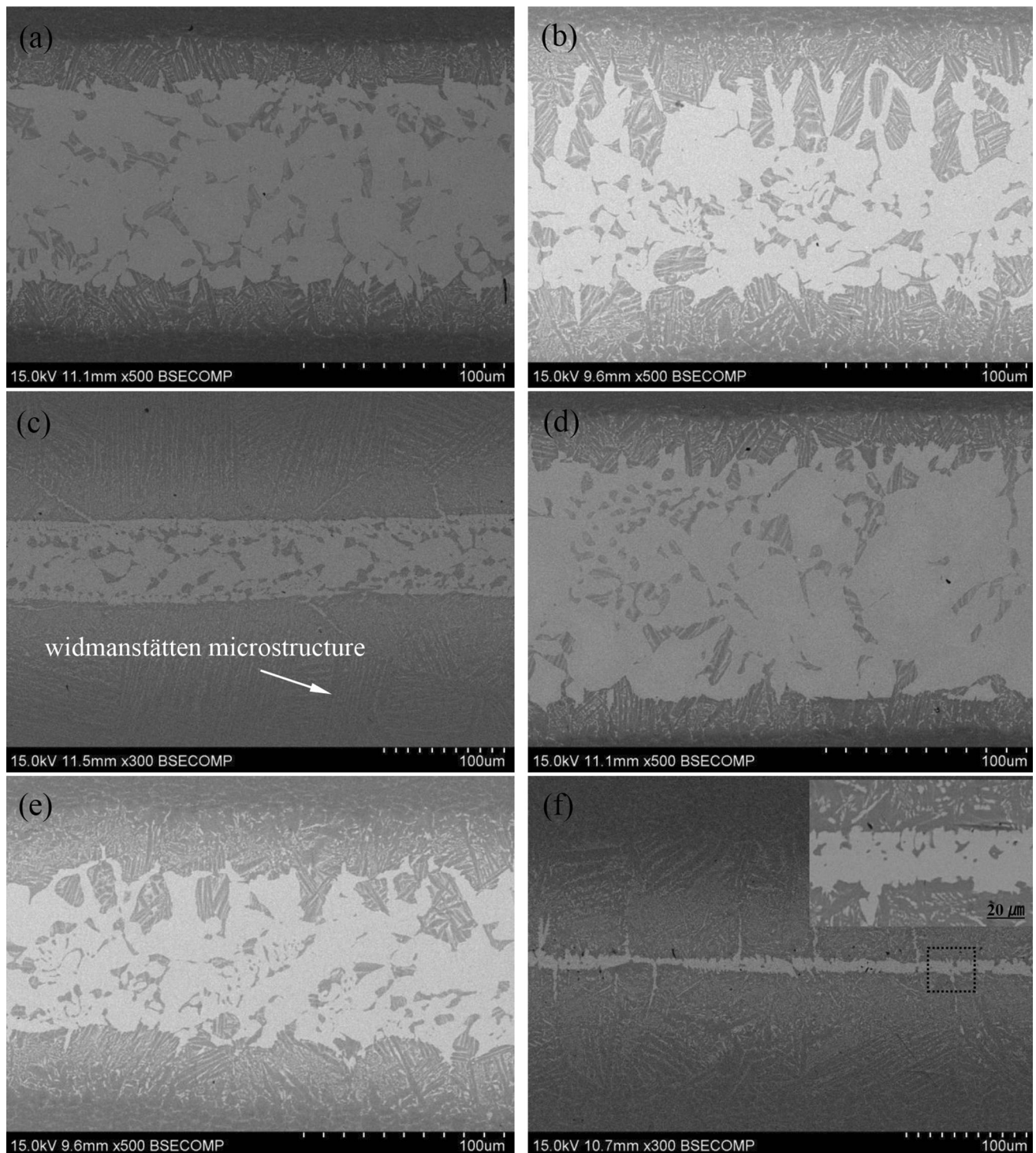
Fig. 4 Microstructure of the brazed joints for: (a) 900°C, 10min; (b) 960°C, 10min; (c) 990°C, 10min; (d) 930°C, 5min; (e) 930°C, 20min; (f) 930°C, 45min

increased from 5 to 45min. The supreme shear strength of brazed joint was 673MPa at 930°C/45min which reached 70% of the based material of TC4 (about 931MPa). That is to say, raising the parameters is beneficial to obtain high strength. But if the brazing temperature is above the β transus temperature of TC4 (985°C), the strength of the based material would dramatically deteriorate. During brazing, it is better to limit the brazing temperature no higher than 985°C. From the result of the microstructure, α-Ti reaction phase had certain toughness. It could prevent the crack propagation and accordingly improve the strength. Therefore, increasing the brazing temperature or lengthening the holding time, the amount of the α-Ti in the center increased which led to the increased shear strength of the joint.
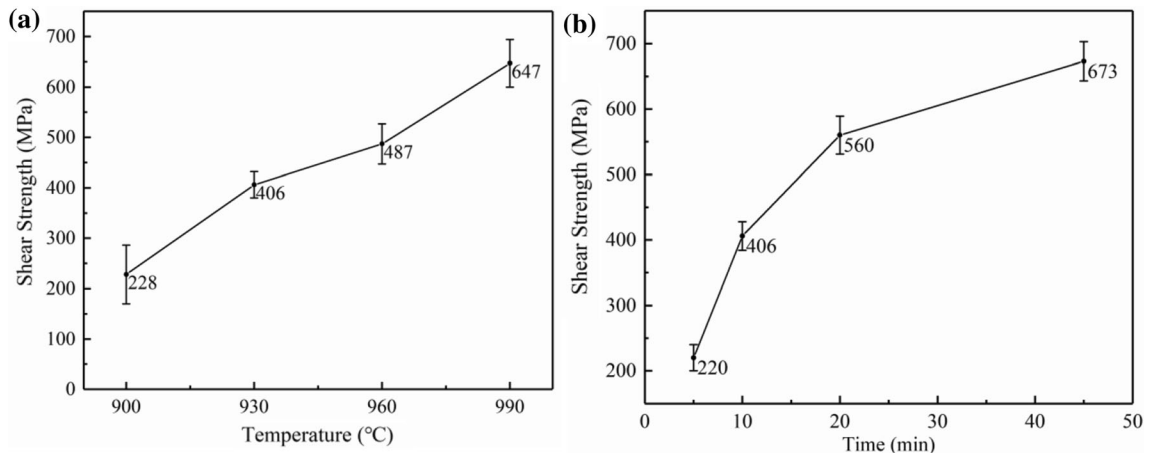
Fig. 5 Effect of (a) brazing temperature (t=10min) and (b) holding time (T=930°C) on shear strength of the brazed joints
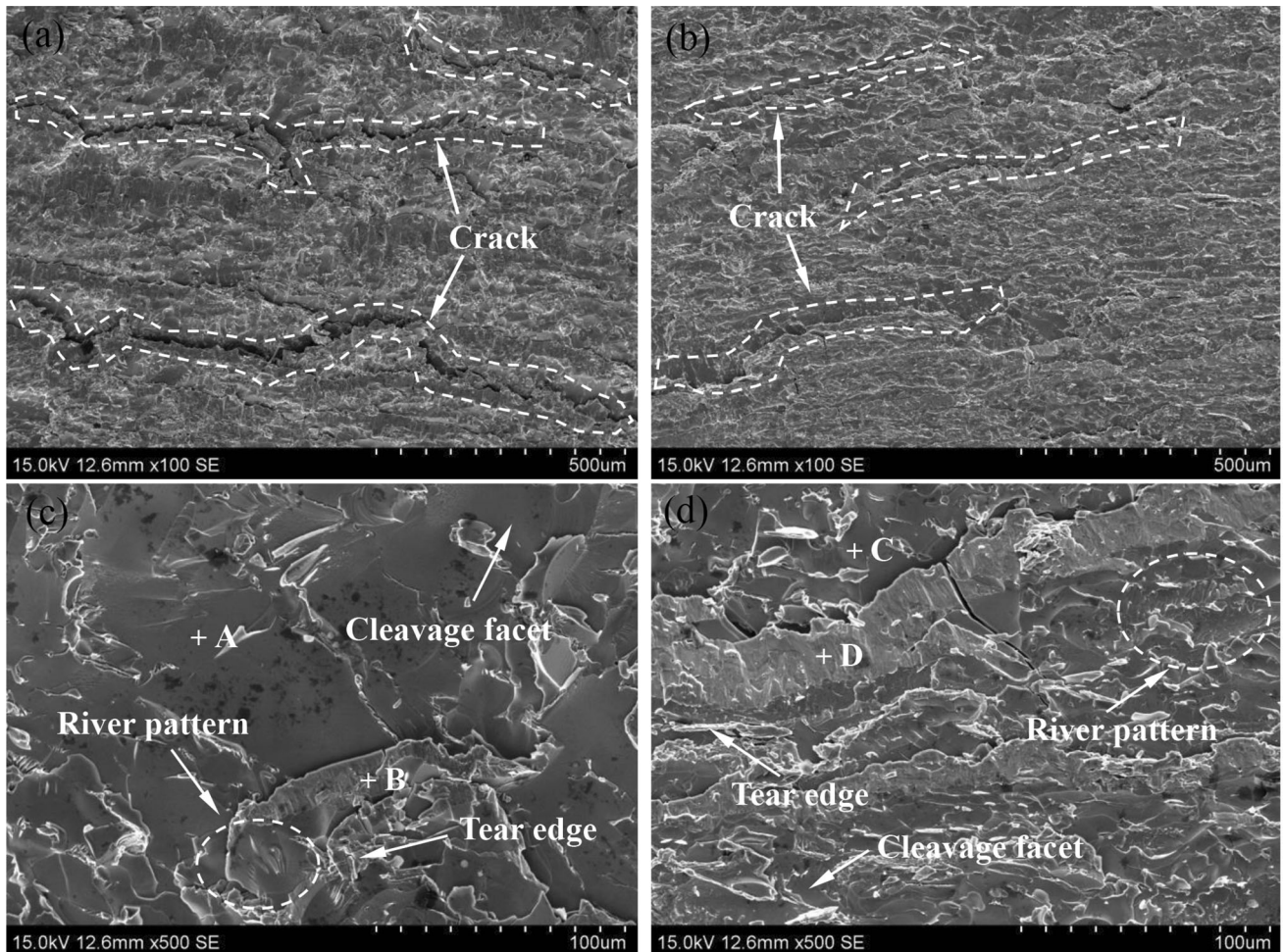
Fig. 6 Fracture morphology of the brazed joints under different brazing parameters: (a) and (c) 900°C, 10 min; (b) and (d) 960°C, 10min

3.3 Analysis of the Fracture Pattern

Figure 6 reveals the fracture morphology of the brazed joints under 900°C and 960°C for 10 min after tensile shear testing. Table 3 gives EDS chemical analysis results of the marked locations. From the high-magnification images of typical fracture morphology in Fig. 6(c) and (d), two fracture patterns were found in the joints: quasi-cleavage and cleavage fracture.

Location A and C expressed cleavage planes and steps. The fracture pattern was typical cleavage fracture, while location B and D consisted in a fine river pattern, tear ridges or step lines. The fracture pattern was quasi-cleavage fracture. From the EDS results in Table 3, location A and C mainly contained Ti, Zr and Ni, and its atomic percentage of (Ti+Zr) and Ni was about 2:1. It was brittle intermetallic compounds ($(Ti,Zr)_2Ni$). From XRD

results (Fig. 7), the fracture surface existed $(Ti,Zr)_2Ni$. Location B and D mainly contained Ti and some Zr and Ni. Combined the microstructure of the brazed joint, it was the eutectoid structure which comprised α-Ti and $(Ti,Zr)_2Ni$. Therefore, the fracture located in zone III. The cracks first nucleated in the big block of brittle $(Ti,Zr)_2Ni$ phase and propagated. When the crack met the α-Ti which was a ductile phase, it may be hindered from propagation. Compared the fracture morphology between 900°C and 960°C, more areas with quasi-cleavage fracture existed at higher brazing temperature. This was consistent with many previous studies (Ref 20-22).

4. Discussion

Figure 8 displays the Ti(Zr)-Ni phase diagram (Ref 23) and a conceptual interface evolution model for the brazed joint by ternary filler metal. Based on Ti(Zr)-Ni phase diagram (Figure 8a), the nucleation and growth mechanisms of reaction phases in the brazing seams were studied. Figure 8(b-f) displays the conceptual microstructural evolution. It contains atomic diffusion characteristics and the formation of reaction phases.

Firstly, physical contact occurs at the interface of based material and the filler metal from the room temperature to the fusion point of the filler metal. When the temperature reaches the fusion point of Ti-Zr-Ni alloy, the filler metal begins to melt. Ti atoms from TC4 partially dissolve into the liquid alloy as Ni and Zr atoms diffuse from the molten alloy into the based material because of the concentration gradient (Fig. 8b).

Then, during the early cooling process after reaching brazing temperature, the hypoeutectic reaction occurs. β-Ti solid solution nucleates and grows up in the TC4/filler metal interface. Moreover, β-Ti is precipitated in the central brazing seam. $\alpha \rightarrow \beta$ phase transformation occurs in the based material near the filler metal. The molten filler metal is changed to solid β-Ti and liquid residual filler metal (Fig. 8c).

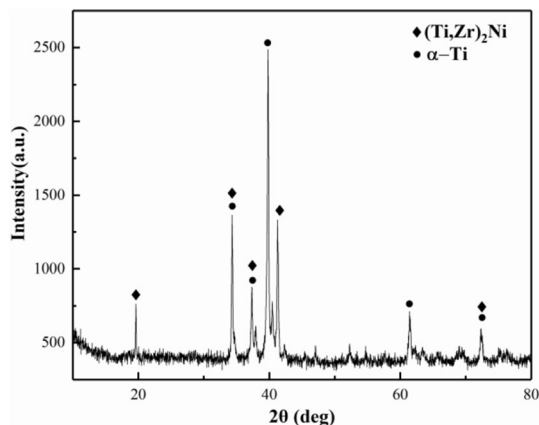Subsequently, solid β-Ti thickens both at TC4/filler metal interface and in the based material close to filler metal. Meanwhile, β-Ti grows up in the central brazing seam. By the time, it declines to the eutectic temperature, and the eutectic reaction of $L \rightarrow \{\beta\text{-Ti}+(Ti,Zr)_2Ni\}_{eutectic}$ occurs in the residual liquid. Consequently, therefore, the central brazing seam consists in big block β-Ti (from precipitated first), tiny β-Ti (from eutectic reaction) and $(Ti,Zr)_2Ni$, as shown in Fig. 8(d).

Finally, the sample continues to cool down. According to Ti(Zr)-Ni phase diagram, all the β-Ti phases transform to α-Ti and $(Ti,Zr)_2Ni$ by eutectoid transformation (β-Ti $\rightarrow$ {α-Ti + $(Ti,Zr)_2Ni$})$_{eutectoid}$. So the microstructures at room temperature: Diffusion zone contains original α-Ti, eutectoid transformation α-Ti and $(Ti,Zr)_2Ni$. Interface zone contains lamellar $(Ti,Zr)_2Ni$ and α-Ti by eutectoid transformation. Center zone contains big block lamellar $(Ti,Zr)_2Ni$ and α-Ti, tiny lamellar $(Ti,Zr)_2Ni$ and α-Ti, together with some $(Ti,Zr)_2Ni$ by eutectic transformation (Fig. 8e).

Besides, during the joining process, Ni atoms enter into the based material (equiaxed α-Ti+intergranular β-Ti) from the melted alloy. Some based material transforms to β-Ti because Ni is a β-Ti stabilized element of TC4. After cooling from high temperature, α-Ti with acicular shape was formed in grain boundary of β-Ti. It may grow along $[110]_\beta$ direction, remaining the untransformed β-Ti. This forms the widmanstätten microstructure. In our experiments, if the heating temperature is above transformation point of β phase (the transformation point of β phase is about 985°C), the diffusion zone eventually forms widmanstätten microstructure (Fig. 8f).

5. Conclusion

TC4 titanium alloy was successfully brazed by Ti-38Zr-24Ni. The microstructure and shear strength of the joint were investigated with variable brazing temperature and holding time. The fractured mode was also studied. Especially the microstructural evolution mechanism of reaction phase was thoroughly discussed. The following are our conclusions:

(1) TC4/TC4 joint consisted of three zones. Diffusion zone consisted of eutectoid structures: α-Ti and $(Ti, Zr)_2Ni$ and remained based material. Interface zone was composed of eutectoid structure: $(Ti, Zr)_2Ni$ and α-Ti. Center zone was comprised of big block brittle $(Ti, Zr)_2Ni$ intermetallic compounds (IMCs) and amounts of big block and tiny eutectoid structure: $(Ti, Zr)_2Ni$ and α-Ti. Increasing the brazing temperature or lengthening the holding time, the breadth of diffusion zone and interface zone increased, but the breadth zone of center zone decreased. Therefore, high brazing temperature or long holding time tended to obtain good quality of the brazed joint.

(2) The highest shear strength of the brazed joint was 673MPa at 930°C/45min, which can reach 70% of the strength of the based material. The shear strength raised with increasing joining parameters due to the decreasing of IMCs in the central of brazing seams.

Table 3 Average chemical compositions (at.%) of different positions in Fig. 6

	Ti	Zr	Ni	V	Al	Possible phase
A	35.41	28.93	32.16	1.48	2.02	$(Ti,Zr)_2Ni$
B	74.81	12.15	6.35	0.75	5.94	eutectoid phases
C	32.75	33.59	31.70	0.59	1.37	$(Ti,Zr)_2Ni$
D	77.47	13.48	5.05	0.80	3.20	eutectoid phases

Fig. 7 XRD analysis of the fracture surface at 900°C for 10 min
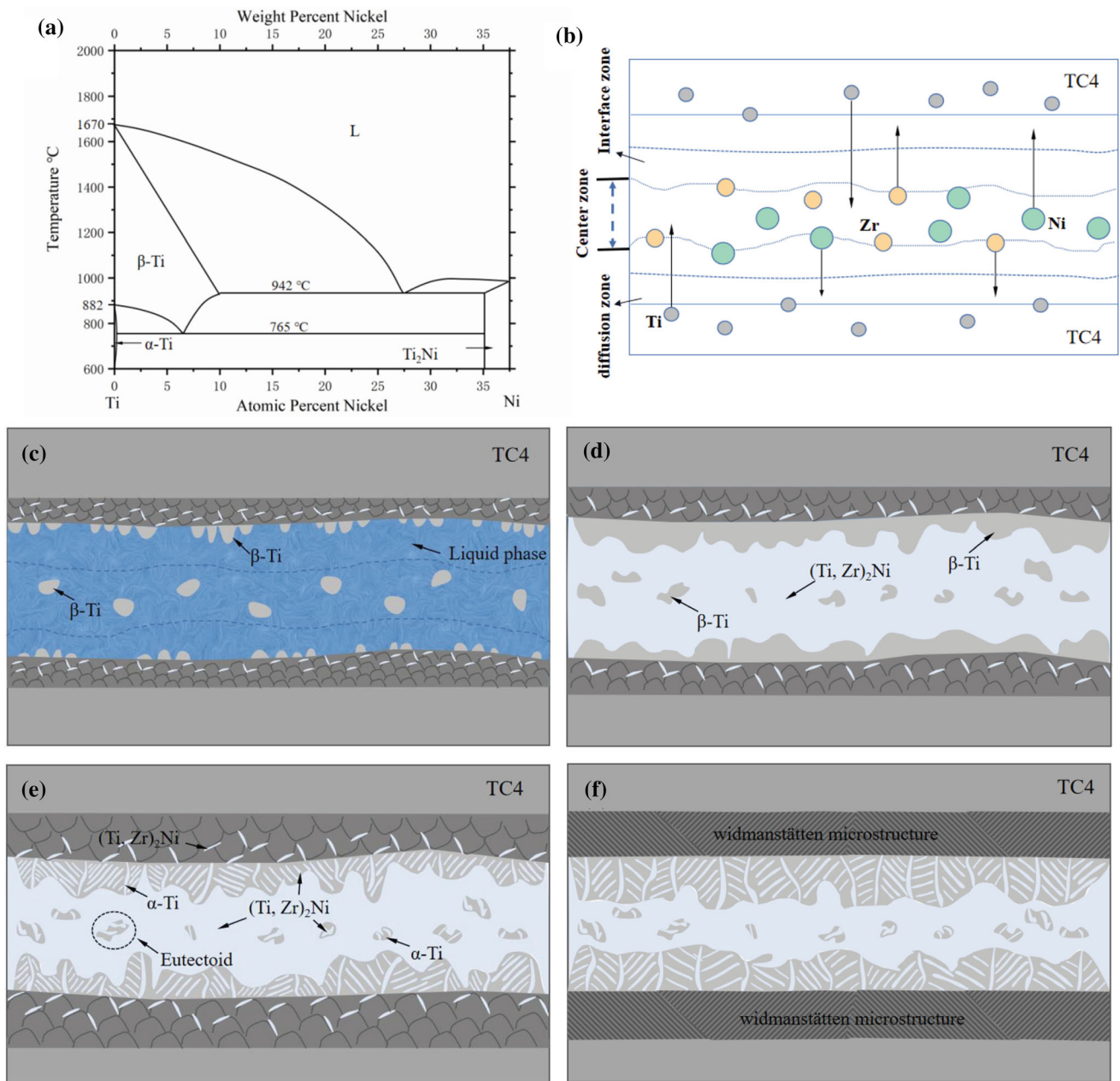
Fig. 8 Ti(Zr)-Ni phase diagram and a conceptual interface evolution model: (a) Ti(Zr)-Ni phase diagram, (b)diffusion (c)-(f) reaction

(3) The fracture took place in the central brazing seam due to existence of brittle $(Ti, Zr)_2Ni$ intermetallic compounds. The cracks tended to generate and propagate in the bulk $(Ti, Zr)_2Ni$ IMCs, but may be hindered by the ductile α-Ti. The fracture surface-expressed two different fracture patterns: quasi-cleavage and cleavage.

References

1. Z.Z. Zou, F.H. Zeng and H.B. Wu, The Joint Strength and Fracture Mechanisms of TC4/TC4 and TA0/TA0 Brazed with Ti-25Cu-15Ni Braze Alloy, *J. Mater. Eng. Perform.*, 2017, **26**, p 2079–2085

2. W.F. Xu, J. Ma and Y.X. Fang, Microstructure and High-Temperature Mechanical Properties of Laser Beam Welded TC4/TA15 Dissimilar Titanium Alloy Joints, *T. Nonferr. Metal. Soc.*, 2020, **130**, p 60–170

3. Y.B. Chen, K.Z. Zhang, X. Hu, Z.L. Lei and L.C. Ni, Study on Laser Welding of a Ti-22Al-25Nb Alloy: Microstructural Evolution and High Temperature Brittle Behavior, *J. Alloys Compd.*, 2016, **681**, p 175–185

4. D.T. Cai, J.C. Chen and C.Y. Hao, Reheat Cracking in Ti2AlNb Alloy Resistance Spot Weldments, *Intermetallics*, 2013, **38**, p 63–69

5. G.J. Feng, Y. Wei, B.X. Hu, Y.F. Wang, D.A. Deng and X.X. Yang, Vacuum Diffusion Bonding of Ti2AlNb Alloy and TC4 Alloy, *T. Nonferr. Metal. Soc.*, 2021, **31**, p 2677–2686

6. E. Chang and C.H. Chen, Low-Melting-Point Titanium-Base Brazing Alloys-Part 1: Characteristics of Two-, Three-, and Four-Component Filler Metals, *J. Mater. Eng. Perform.*, 1997, **6**, p 792–796

7. Y. Peng, J.L. Li and Y.J. Du, Microstructure and Mechanical Properties of Joints Prepared by Vacuum Brazing on TC4 Titanium Alloy with Ag as Filler Metal, *Vacuum*, 2021, **187**, 110134

8. D. Dong, D.D. Zhu and H.X. Zheng, Brazing TiC/Ti Matrix Composite Using Ti-Ni Eutectic Braze Alloy, *Vacuum*, 2018, **156**, p 411–418

9. L.L. Sun, S.J. Pang and Y. Liu, A Ti-Zr-Cu-Ni-Co-Fe-Al-Sn Amorphous Filler Metal for Improving the Strength of Ti-6Al-4V Alloy Brazing Joint, *Prog. Nat. Sci. Mater.*, 2017, **27**, p 687–694

10. O. Botstein and A. Rabinkin, Brazing of Titanium-Based Alloys with Amorphous 25wt.%Ti-25wt.%Zr-50wt.%Cu Filler Metal, *Mater. Sci. Eng. A.*, 1994, **188**, p 305–315

11. Y.J. Jing, H.P. Xiong, Y.L. Shang, J.S. Wang, Y.Y. Cheng and J. Jiang, Design TiZrCuNi Filler Materials for Vacuum Brazing TA15 Alloy, *J Manuf Process.*, 2020, **53**, p 328–335

12. C.T. Chang, R.K. Shiue and C.S. Chang, Microstructural Evolution of Infrared Brazed Ti-15-3 Alloy Using Ti-15Cu-15Ni and Ti-15Cu-25Ni Fillers, *Scripta Mater*, 2006, **54**, p 853–858

13. C.T. Chang, Y.C. Du and R.K. Shiue, Infrared Brazing of High-Strength Titanium Alloys by Ti-15Cu-15Ni and Ti-15Cu-25Ni Filler Foils, *Mater. Sci. Eng. A.*, 2006, **420**, p 155–164

14. M.K. Lee and J.G. Lee, Mechanical and Corrosion Properties of Ti-6Al-4V Alloy Joints Brazed with a Low-Melting-Point 62.7Zr-11.0Ti-13.2Cu-9.8Ni-3.3Be Amorphous Filler Metal, *Mater. Char.*, 2013, **81**, p 19–27

15. S.J. Pang, L.L. Sun and H.P. Xiong, A Multicomponent TiZr-Based Amorphous Brazing Filler Metal for High-Strength Joining of Titanium Alloy, *Scripta. Mater.*, 2016, **117**, p 55–59

16. A. Shapiro and A. Rabinkin, State of the Art of Titanium-Based Brazing Filler Metals, *Weld. J.*, 2003, **82**, p 36–43

17. Y. Wang, M. Jiao and Z.W. Yang, Vacuum Brazing of Ti2AlNb and TC4 Alloys Using Ti-Zr-Cu-Ni and Ti-Zr-Cu-Ni Plus Mo Filler Metals: Microstructural Evolution and Mechanical Properties, *Arch. Civ. Mech. Eng.*, 2018, **18**, p 546–556

18. L. Li, X.Q. Li and M. Hu, Effects of Brazing Temperature and Testing Temperature on the Microstructure and Shear Strength of γ-TiAl Joints, *Mater. Sci. Eng. A.*, 2015, **634**, p 91–98

19. I.T. Hong and C.H. Koo, Microstructural Evolution and Shear Strength of Brazing C103 and Ti-6Al-4V Using Ti-20Cu-20Ni-20Zr (wt.%) Filler Metal, *Int. J. Refract. Met. H.*, 2006, **24**, p 247–252

20. E. Ganjeh, H. Sarkhosh and M.E. Bajgholi, Increasing Ti-6Al-4V Brazed Joint Strength Equal to the Base Metal by Ti and Zr Amorphous Filler Alloys, *Mater. Char.*, 2012, **71**, p 31–40

21. Y.S. Cai, R.C. Liu and Z.W. Zhu, Effect of Brazing Temperature and Brazing Time on the Microstructure and Tensile Strength of TiAl-Based Alloy Joints with Ti-Zr-Cu-Ni Amorphous Alloy as Filler Metal, *Intermetallics*, 2017, **91**, p 35–44

22. P. He, J.C. Feng and H. Zhou, Microstructure and Strength of Brazed Joints of Ti3Al Base Alloy with Ti-Zr-Ni-Cu Filler Metal, *Mater. Sci. Eng. A.*, 2005, **392**, p 81–86

23. H. Donthula, B. Vishwanadh and T. Alam, Morphological Evolution of Transformation Products and Eutectoid Transformation(s) in a Hyper-Eutectoid Ti-12 at% Cu Alloy, *Acta. Mater*, 2019, **168**, p 63–75